Brain Research, 534 (1990) 15–24
Elsevier

BRES 16060

Hair cell tufts and afferent innervation of the bullfrog crista ampullaris

Steven F. Myers and Edwin R. Lewis

Department of Otolaryngology 5E-UHC, Wayne State University School of Medicine, Detroit, MI 48201 and Department of Electrical Engineering and Computer Sciences, University of California, Berkeley, CA 94720 (U.S.A.)

(Accepted 5 June 1990)

Key words: Semicircular canal; Hair cell; Vestibular afferent neuron

Within the bullfrog semicircular canal crista, hair cell tuft types were defined and mapped with the aid of scanning electron microscopy. Intracellular recording and Lucifer Yellow labeling techniques were used to study afferent responses and arborization patterns. Dye-filled planar afferent axons had mean distal axonal diameters of 1.6–4.9 μm, highly branched arbors, and contacted 11–24 hair cells. Dye-filled isthmus afferent axons had mean distal axonal diameters of 1.8–7.9 μm, with either small or large field arbors contacting 4–9 or 25–31 hair cells. The estimated mean number of contacts per innervated hair cell was 2.2 for planar and 1.3 for isthmus afferent neurons. Data on evoked afferent responses were available only for isthmus units that were observed to respond to our microrotational stimuli (<3°/s peak rotational velocity). Of 21 such afferent neurons, 8 were successfully dye-filled. Within this small sample, high-gain units had large field arbors and lower-gain units had small field arbors. The sensitivity of each afferent neuron was analyzed in terms of noise equivalent input (NEI), the stimulus amplitude for which the afferent response amplitude is just equivalent to the RMS deviation of the instantaneous spike rate. NEI for isthmus units varied from 0.63 to 8.2°/s; the mean was 3.2°/s.

INTRODUCTION

Afferent neurons innervating the semicircular canal organs of the vertebrate inner ear exhibit a wide range of physiological characteristics. Attempts to discover the bases for this variability are continuing and have lead to studies that combine quantitative neurophysiological and anatomical methods[1,11,13]. Results from these as well as earlier studies have divided the crista neuroepithelium into central and peripheral regions based on general anatomical features, differences in afferent fiber sizes and conduction speeds, as well as differences in afferent fiber response gains, spontaneous activity and the regularity of the spontaneous activity[1,5,6,11,13]. The vertical canal cristae have been described as dumbbell or saddle shaped with 2 enlarged 'planar expansions' curving along the ampullar wall (Fig. 1). The horizontal crista resembles that of a halved vertical canal crista. The isthmus region between the planar expansions of the vertical canals is raised centrally from the floor of the ampulla, forming the crista ridge. The peripheral regions of the frog crista comprise the neuroepithelia of the planar expansions and possibly 1 or 2 sparsely populated rows of hair cells along the perimeter of the neuroepithelium of the isthmus region. The more centrally placed neuroepithelium of the crista ridge is considered the central region. Mammalian cristae differ from the vertical canal crista of frogs by having substantially more hair cells occupying the sides of the crista ridge. Based primarily on hair cell density differences, Lindeman[16] distinguished 3 epithelial zones (central, peripheral and intermediate) of approximately equal areas in mammalian preparations (see also ref. 3).

Hillman[8] and Li and Lewis[14] recognized 2 types of hair cell tufts on the crista ampularis of the American bullfrog *Rana catesbeiana*. These tuft types were designated as mature and immature types by Li and Lewis, with the immature type found primarily on the perimeter of the epithelium where new cells are added during growth. Flock and Orman[4] subdivided the mature hair cell tuft population into 2 types in the european grass frog, *Rana temporaria* with somewhat overlapping distributions along the crista.

The goals of the current study were the following: (1) to determine whether this same subdivision of the mature hair cell tuft population exists in the American bullfrog; (2) if so, to determine whether these mature tufts follow the same regional distributions; (3) if so, to determine by dye tracing studies whether or not innervation patterns respect the boundaries of these regions; (4) in general, to determine by dye-tracing studies whether or not there are functional variations among axons that depend on innervation pattern but are independent of the region inner-

Correspondence: S.F. Myers, Department of Otolaryngology 5E-UHC, Wayne State University School of Medicine, 540 East Canfield, Detroit, MI 48201, U.S.A., Tel. (313)745-4648.

vated. While the emphasis in this study was on the anterior canal crista, some data are also shown for the horizontal canal crista.

MATERIALS AND METHODS

Crista morphology

To obtain more quantitative information on the neuroepithelia of the canal cristae, measurements were taken from whole mount preparations, light-microscopic histological sections and scanning electron micrographs of the cristae from three 60–65 g bullfrogs (snout/vent length = 9 cm). The frogs were anesthetized with sodium pentobarbital (60 μg/g body weight), decapitated, the otic capsules opened and perfused with a solution containing 4% paraformaldehyde and 2% glutaraldehyde in 0.1 M phosphate buffer (pH 7.4). The membranous labyrinth was then removed, placed in fresh fixative solution of the same composition, and partially dissected to improve fixation of internal structures. After 1 h the tissues were rinsed in buffer, postfixed for an additional hour in 1% osmium tetroxide in buffer. Subsequent fine dissection was carried out in 70% ethanol, the tissues were further dehydrated and critical point dried in CO_2, mounted on stubs, coated with platinum and viewed in an Amray 1000 SEM. For histological sectioning dehydrated tissues were embedded in plastic resin and 3-μm sections made with glass knives on a Sorvol MT2-B Ultramicrotome.

Afferent arborizations and physiology

Surgical and electrophysiological techniques are described in detail elsewhere[18]. Briefly, bullfrogs, *Rana catesbeiana*, weighing 50–180 g were anesthetized with either sodium pentobarbital alone (60 μg/g body weight, i.m.) or in combination with ketamine hydrochloride (30 μg/g of each anesthetic) with supplemental injections as necessary. The VIIIth nerve was approached through the roof of the mouth. The activity of single vestibular nerve fibers was recorded intra-axonally with single-barrelled glass micropipettes containing a 5% (w/w) solution of the fluorescent dye Lucifer Yellow[20] in distilled water. In one set of experiments, in which evoked responses were not studied, electrode penetrations of the anterior canal nerve were made via an intra-labyrinthine approach. Prior to dye-filling, the penetrated units were characterized by the regularity of their resting spike rate. In the second set of experiments, the VIIIth nerve was exposed within the cranial cavity leaving the otic capsule intact. Each frog was then positioned ventral side up on a servo-driven tilt table with the axis of the anterior vertical canal congruent with the axis of tilt. Penetrated afferent axons were selected for recording/dye-filling on the bases of their responses to a 0.4° peak to peak, 0.5-Hz sinusoidal tilt stimulus which would be expected to select for the more sensitive units. Spike activity was recorded for 2–3 min for resting activity and for each of several sinusoidal tilt stimuli, usually followed by an additional period of resting activity. Regularity of resting discharges was quantified using the coefficient of variation (CV) in interspike interval[6,11]. One canal dye-fill was attempted per frog.

Reconstructions of afferent arbors were made from dissected, formalin-fixed tissues which were cleared in methyl salicylate, mounted in depression slides and viewed with a Zeiss Universal microscope with fluorescence attachments. Terminal arborizations of dye-filled neurons were sketched against an eye piece graticle using a 100 × oil immersion objective. Axonal diameter measurements of dye-filled afferent neurons represent internal axonal diameters corrected for tissue shrinkage.

Afferent sensitivity was quantified in terms of response gains as well as the noise equivalent input (NEI) for units with mean resting spike rates of 2.5 spikes/s or greater. NEI is a conventional method used by transducer engineers to distinguish between the *gain* of a sensor and its *sensitivity*, with the latter taking into account the noise associated with the sensor. In studies of neural responses, NEI can be defined as the stimulus level (in degrees/s) that would evoke a spike rate response peak just equal to the root mean square (RMS) variation in spontaneous instantaneous spike rate (ISR). The ISR is simply the reciprocal of the interspike interval. We take this variation to be a reflection of the noise associated with the axon and with its peripheral sensory structures. The NEI can be estimated by dividing the standard deviation of the ISR by the gain of the afferent neuron (spikes/s per degree/s):

$$\mathrm{NEI} = \frac{\mathrm{SD}}{gain} = \frac{\frac{1}{n-1}\sqrt{\sum_{i}^{n}(x_i-\bar{x})^2}}{gain}$$

where n = the total number of 'instantaneous spike rates' (ISR = 1/interspike interval in seconds), x_i = the value of the i th ISR, $\bar{x}$ = the mean instantaneous spike rate, SD = the standard deviation of $\bar{x}$, and *gain* = spikes/s per degree/s.

For regularly discharging neurons, the RMS noise-induced variation of individual units can be estimated indirectly from the mean and standard deviations of the interspike interval statistics. This is accomplished by determining the values of the interspike interval one standard deviation above and below the mean interval, then converting to the ISR equivalent values. This range, divided by 2, is a good approximation of the RMS deviation of the ISR, if the resting afferent discharge is regular (CVs < 0.35).

RESULTS

Bullfrog crista morphology

Scanning electron micrographs of the vertical and horizontal canal cristae are shown in Fig. 1. We found general features of the cristae to conform well to previous descriptions[7,9,14]. It was noteworthy that although the horizontal crista shape resembled that of a halved vertical canal crista it was roughly 2/3rds the length of a vertical canal crista, with a disproportionately large planar region.

Measurements of neuroepithelial surface areas and estimates of hair cell densities were based on crista measurements corrected for shrinkage during tissue processing. Tissue shrinkage due to the fixation step (primary + post-fixation) was estimated to be 3% from whole mount preparations of tissues from an additional animal used solely for this purpose. The vertical canal cristae after fixation measured 800 ± 15 μm (n = 6) in whole mount preparations prior to dehydration. Correcting for 3% fixation shrinkage gave an unfixed mean crista length of approximately 825 μm. After dehydration the cristae were 665 ± 10 μm long, for a total shrinkage of 20%. Cristae from one ear of each animal were embedded in epoxy resin and sectioned for light-microscopic examination. Sections through the length of the crista demonstrated no additional shrinkage due to the embedding process. Measurements taken from scanning electron micrographs and confirmed by measurements of the SEM specimens taken under a stereo microscope showed a crista length of 525 ± 8 μm (n = 4) for a total shrinkage from prefixation dimensions of 36% for non-embedded, critical-point-dried specimens.

Due to the sharp slope of the planar expansions up the wall of the ampulla, the length along the surface contour of a vertical canal crista (estimated from scanning electron micrographs and verified by light-microscopic examination of one S.E.M. preparation after dividing it in half longitudinally with a razor blade) was approximately 11% greater than the length of the crista projected onto the plane of a micrograph. The horizontal canal crista is flatter so that the length of the surface contour was only about 4% greater than the projected measurement.

With these considerations in mind, estimates were made of regional neuroepithelial surface areas (Fig. 2). A boundary between the planar region and the isthmus, though lacking precise land marks, was defined as a line across the crista where an abrupt change in the general character of the ciliary tufts (due to the relative lengths, thicknesses, and numbers of the stereocilia in different tufts) and the hair cell density produce the appearance of a regional boundary just beyond the point at which the crista begins to expand and slope upward (see Fig. 1). For the vertical canal crista this boundary line was located at 17% of the surface contour distance from the ends of the crista. For the horizontal canal crista this line was located at 34% of the surface contour distance from the planar end of the crista. Based again on general tuft character along with some widening of the crista neuroepithelium centrally, the isthmus regions can be further subdivided. The boundaries formed by the subdivisions divide the crista of the horizontal canal roughly in half and the crista of vertical canal crista roughly in thirds. This separates out the slightly raised torus region (zone III) from the arms of the isthmus (zone II) connected to the planar expansions. Based on these estimates of regional boundaries, the planar sensory surface areas for vertical and horizontal canal crista were very similar, 87 000 and 80 000 μm^2, respectively. The subdivisions of the isthmus regions for both the vertical and horizontal canal crista are of approximately equal length, however, the horizontal canal isthmus was roughly 12% broader than its vertical canal counter part. So, although the vertical canal isthmus was 33% longer than the horizontal canal 'isthmus', it had only 25% more total surface area (68 000 μm^2 vs. 54 000 μm^2).

The density of hair cells in the planar regions was approximately twice that of the isthmus region. It was also apparent that the hair cell density was somewhat less along the midline of the crista, at least for the isthmus and the adjacent half of the planar expansion. Sample hair cell counts made from scanning electron micrographs gave average numbers of hair cells within a surface area of 5000 μm^2 of 65 for planar and 33 for isthmus regions of both vertical and horizontal canal cristae. Based on the estimates of total surface areas, projected total numbers of planar vs. isthmus hair cells were 1100 and 450 for the vertical canals, and 1000 and 350 for the horizontal canals.

Hair cell tufts

Examination of hair cell tuft morphology along the crista revealed a pattern similar to that described for *Rana temporaria* by Flock and Orman[4]. Ciliary tufts, in frogs, generally have a single 65–70 μm long kinocilium and lack the regional variability in kinocilia length seen in mammalian crista[15]. Hair cell tuft types can be differentiated on the basis of stereocilia length, thickness and number. The tuft types in Fig. 3 are shown for illustrative purposes without their kinocilia. Using the nomenclature of Flock and Orman, the type A tufts were characterized by a long row of 5–6 stereocilia of approximately the same length as the kinocilium. The type B tufts had relatively thinner stereocilia of which a long row of 4–6 stereocilia generally extended less than 2/3rds of the length of the kinocilium. The secondary rows of the type B tufts were also considerably shorter and often fewer in number than their counter parts in a typical type A tuft. However, the type B tuft represents a less distinct group with gradations in stereocilia lengths and thickness, becoming longer and thicker away from the perimeter of the neuroepithelium. The 1 or 2 rows of type C tufts along the perimeter were characterized by short stereocilia, the longest often less than 5 μm but approaching 15 μm in some cases.

As in Flock and Orman's study, the planar expansions (zone I) of the bullfrog crista contained no type A tufts while the isthmus (zones II and III) contained a mix of type A and B tufts. One possible difference in the bullfrog is that region III of the isthmus was populated almost exclusively with type A tufts. This allows the isthmus region of the bullfrog to be subdivided morphologically into a type A region and a mixed A-B region.

Based on these distributions and measurements of hair cell densities, the type A tuft, which is mostly restricted to region III, represents only 11–12% of the total hair cell population. The majority of hair cells (72–74%) are located on the planar expansions and nearly all of these have type B tufts. The remaining approximately 15% comprise hair cells with type C (immature) tufts.

Afferent nerve fibers

In one set of experiments, in which evoked responses were not studied, 14 successful dye-fills were made (Fig. 4). Of these units, 6 had regular spike discharge patterns (CVs $\cong$ 0.2), mean spike rates of 6–20 spikes/s, and terminal arbors limited to the planar regions of the crista. The mean distal axonal diameter of these afferent neurons was 3.0 μm (range 1.5–4.9; S.D. 1.0). Estima-

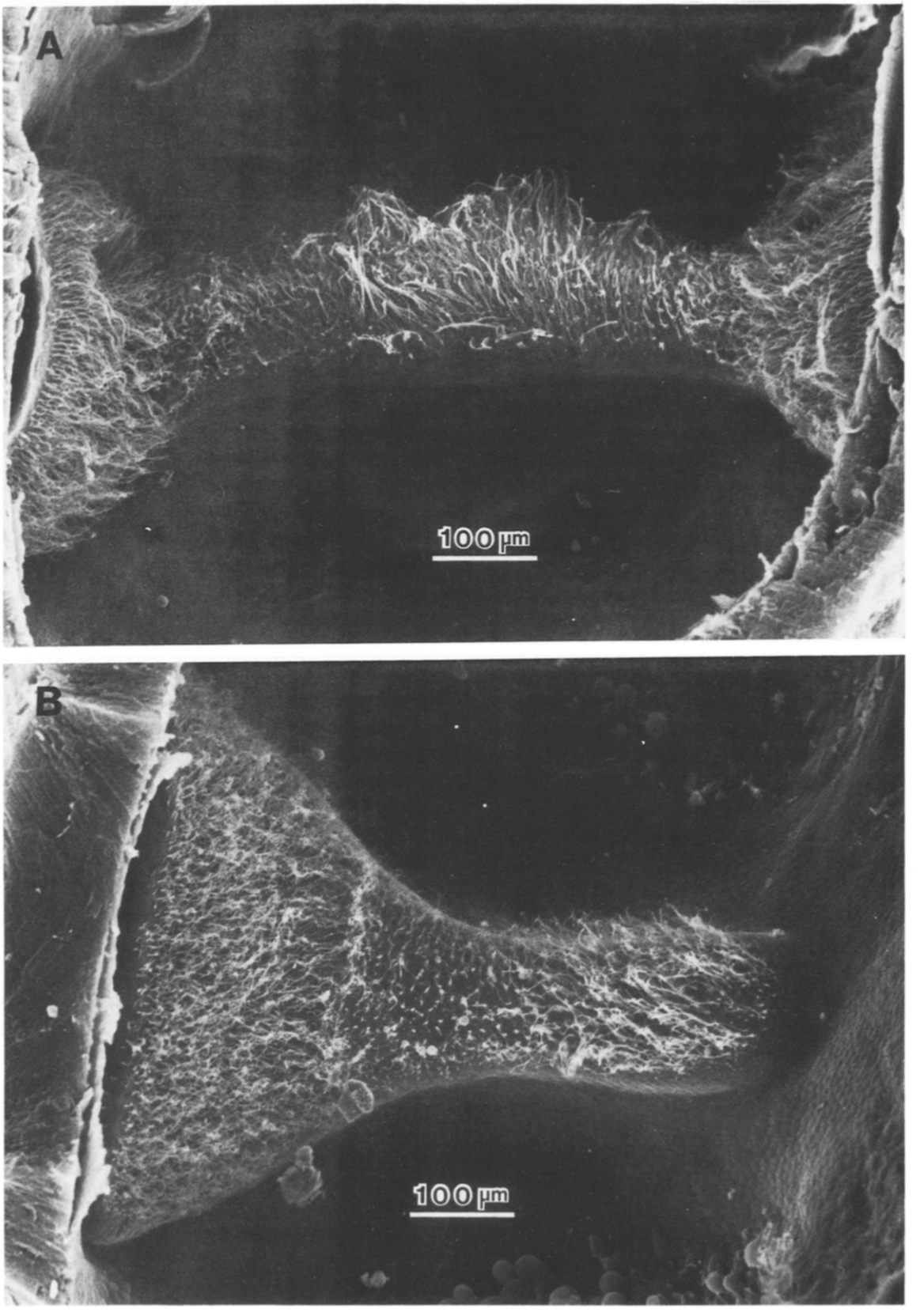

Fig. 1. Low-power scanning electron micrographs showing regional variation of hair cell tufts along the crista. A: anterior canal crista; B: horizontal canal crista.

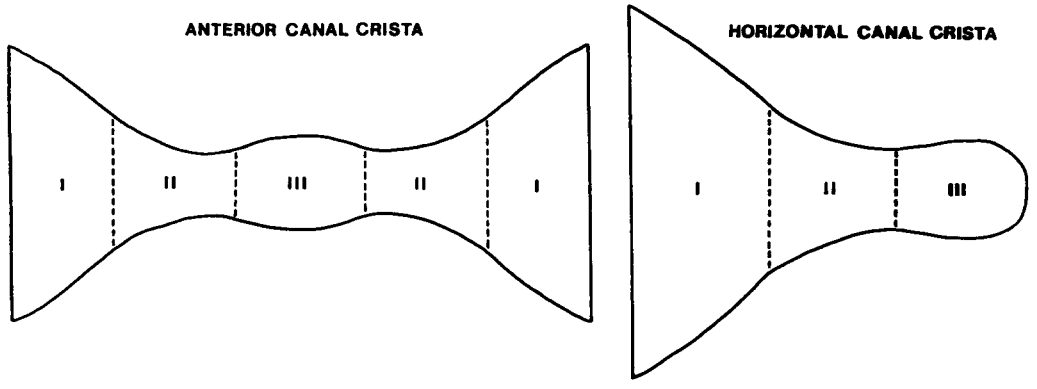

Fig. 2. Diagram illustrating regional divisions of neuroepithelium (see text).

tion of the myelin sheath contribution (approximately 0.5 times axonal diameter; see ref. 13) would add 0.75–2.5 μm to the total fiber diameter. This indicates that these dye-filled axons were representative of larger caliber planar afferent fibers (2–10 μm) and *not* representative of the majority of planar axons (60%) that have total nerve fiber diameters of 2 μm or less[12]. The remaining 8 fibers terminated in the isthmus region of the crista.

In a second set of experiments where resting and evoked responses were recorded from 21 units, 8 additional units were successfully dye-filled, and all terminated in the isthmus region. The criterion for selecting responding axons (see Materials and Methods section) favored those with high gain. Based on previous work, one would expect high gain axons to originate in the isthmus region[11,13]. All 21 of these isthmus-afferent axons plus the 8 other isthmus dye-filled axons from the first set of experiments had irregular resting discharge patterns, with coefficients of variation in interspike interval (CV) ranging from 0.59–0.9. The resting spike rate for all 29 irregular units ranged from 0.8 to 15.4 spikes/s with 45% in the range above 9 spikes/s, 48% between 2 and 7 spikes/s and 7% (2 units) with spike rates less than 1. These values contrast with those for the 6 planar units where 50% had resting spike rates above 14 spikes/s and only one (17%) had a resting spike rate less than 9 spikes/s. A total of 16 isthmus and 6 planar dye-filled, afferent axons were available for morphological analysis. In general, if the fluorescent dye could be traced all the way into the neuroepithelium, the terminal arborizations could be easily traced even in relatively faint fills unless the background fluorescence was unusually intense. This was the case in 2 instances (Fig. 5C,F) where the dye-fill may have extended beyond where it could be seen under fluorescence microscopy.

Afferent arborizations in the isthmus region were divisible into large-field or small-field patterns (Figs. 5 and 6). Large field arbors (LFA) extended 180–340 μm along the crista, contacting 24–31 hair cells (Fig. 7). Often many hair cells within a large field unit's area of innervation were not contacted by that afferent neuron. Small field arbors (SFA) were 70–140 μm in extent, contacting 4–9 hair cells, usually in close proximity to each other. Planar units (PA) had much more restricted arbors with circular or oblong fields, 40–70 μm in diameter and contacting 11–24 hair cells. Dendritic 'contacts' were judged from whole mount preparations using fluorescence microscopy and should not be inter-

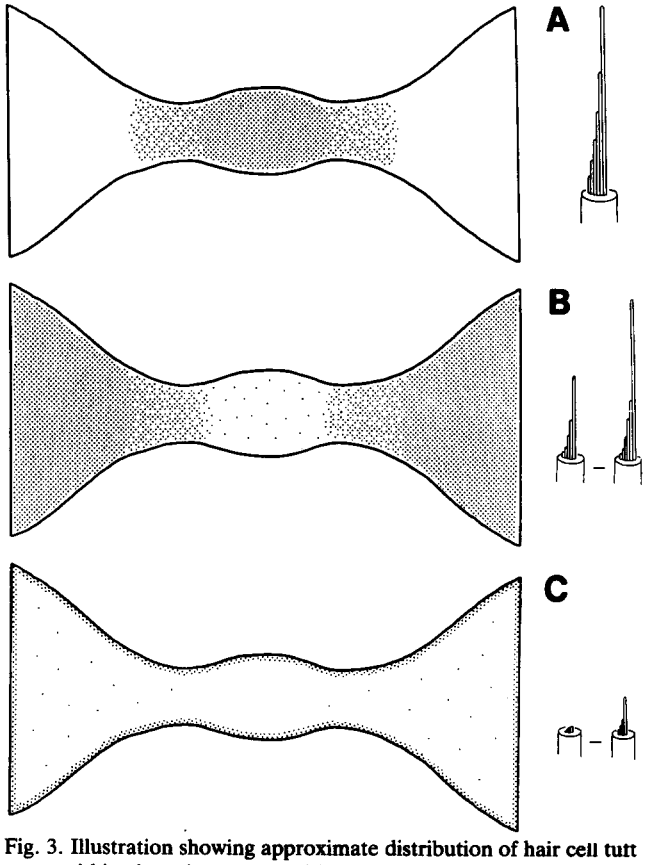

Fig. 3. Illustration showing approximate distribution of hair cell tuft types within the crista neuroepithelium. Tuft types are illustrated *without* their kinocilia to emphasize stereocilia differences. Note range of morphology for tuft types B and C.

preted as necessarily implying synaptic connections. The determination of a contact was made either by a dendritic branch ending adjacent to a hair cell body or by a bouton-like enlargement at the end of a dendritic branchlet immediately adjacent to a hair cell body, or along a branchlet as it passed very close to a hair cell body. Often the terminal branchlets could be followed up the side of the hair cell.

Axonal diameters

Axonal diameters near the crista were always smaller than those proximal to the cell body, in some cases only by 5–10% but more often by 25–50% and in 1 case 67%. This reduction in axonal diameter usually occurred fairly abruptly just distal to the cell body or within the next 50–60 μm. The proximal dye-fill profile was sometimes quite irregular which on histological sectioning appeared to be due to vacuoles produced during fixation. However, the myelin sheath profile was not distorted and internal (axonal) diameters could be measured easily. The distal axon always had a relatively smooth profile which generally tapered distally. In a few cases this tapering was quite marked, representing a 20–36% reduction in axonal diameter distally. In 10 out of the 19 dye-fills in which measurements of distal processes were made, the tapering was less than 10% and in 3 cases there was no apparent tapering. For comparisons between dye-filled units, axonal diameters reported below represent the mean of distal axonal diameters taken proximal, beneath and distal to the utricle.

The largest diameter dye-filled axon belonged to the LFA group. The two smallest diameter axons were planar units. However, overall the axonal diameters of the LFA, SFA and PA dye-fills were not significantly different and there was no correlation between axonal diameter and number of hair cells contacted (Fig. 8A). The apparent number of contact points per hair cell made by isthmus units was very similar regardless of the size of arbor (LFA: 1.29 contacts/hair cell, n = 6, S.D. = 0.08; SFA: 1.3 contacts/hair cell, n = 9, S.D. = 0.20). However, as

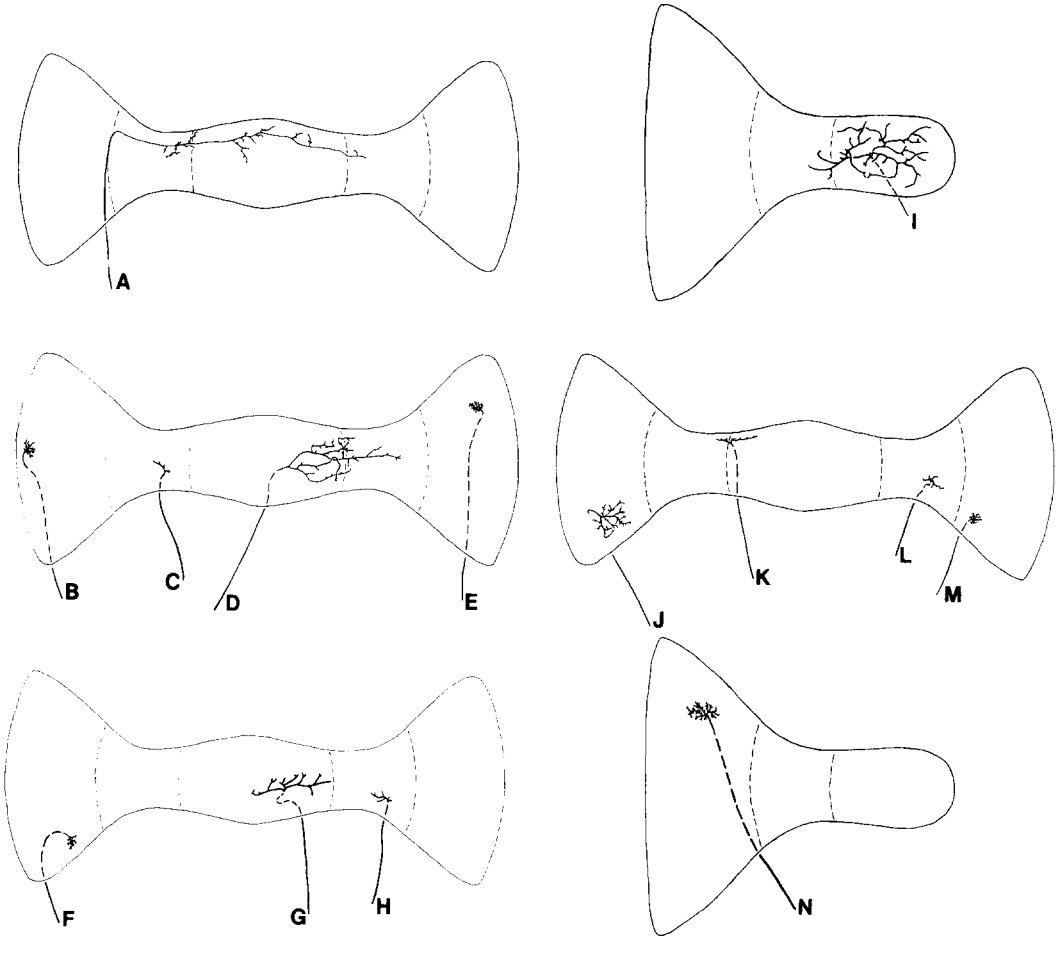

Fig. 4. Examples of afferent arborizations demonstrated by Lucifer Yellow dye-filling from an intralabyrinthine approach. Mean distal axonal diameters for these afferents were (in order): 3.6, 1.6, 3.4, 7.9, 1.6, 3.4, 3.5, 2.2, 2.5, 4.8, 5.4, 2.5, 2.5, 4.0 μm. Afferent E was unique in its distinct 'bunch-of-grapes' appearance. Afferent C and F had relatively low fluorescence compared to the background auto-fluorescence of the labyrinthine tissues such that completeness of dye tracing was more questionable than the other dye-fills.

shown in Fig. 7B, the mean number of contacts per hair cell made by planar afferent neurons (2.15 contacts/hair cell, n = 6, S.D. = 0.16; see Fig. 8B) was significantly greater statistically than the number of contacts per hair cell made by isthmus afferent neurons ($P < 0.005$; Student's t-test).

Afferent arborizations to the isthmus region often crossed the boundaries between zones II and III. This was generally not the case for the boundary between zones I and II. One apparent exception was found (Fig. 6H). This afferent neuron had an arbor similar to the dye-filled planar units, contacting 17 hair cells (see Fig. 7A,B) and had the lowest gain of all the microrotationally sensitive afferent axons studied (0.4 spikes/s per deg/s to a 0.5 Hz stimulus). However, the mean number of afferent contacts per hair cell was 1.24, and the resting spike rate of this unit was markedly irregular (CV = 0.9), both findings characteristic of isthmus units.

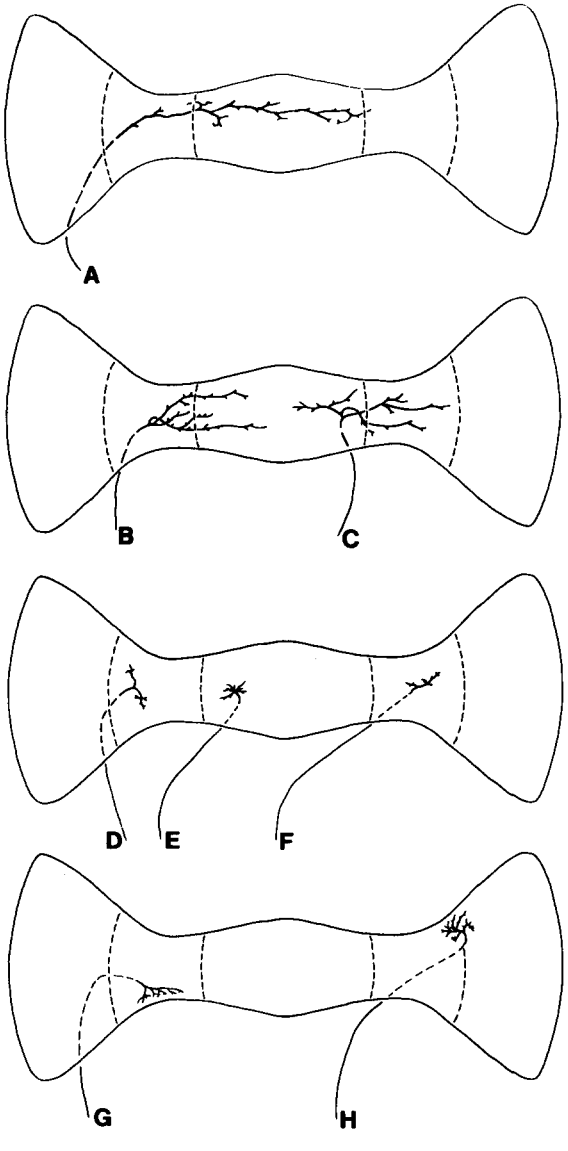

Fig. 5. Illustrations of 8 dendritic arbors from dye-fills in which evoked responses were also studied. A–C: high gain units; D–H: lower gain units. Mean distal axonal diameters for these afferents were (in order): 2.0, 1.8, 2.9, 3.9, 2.5, 4.6, 4.6, 3.5 μm.

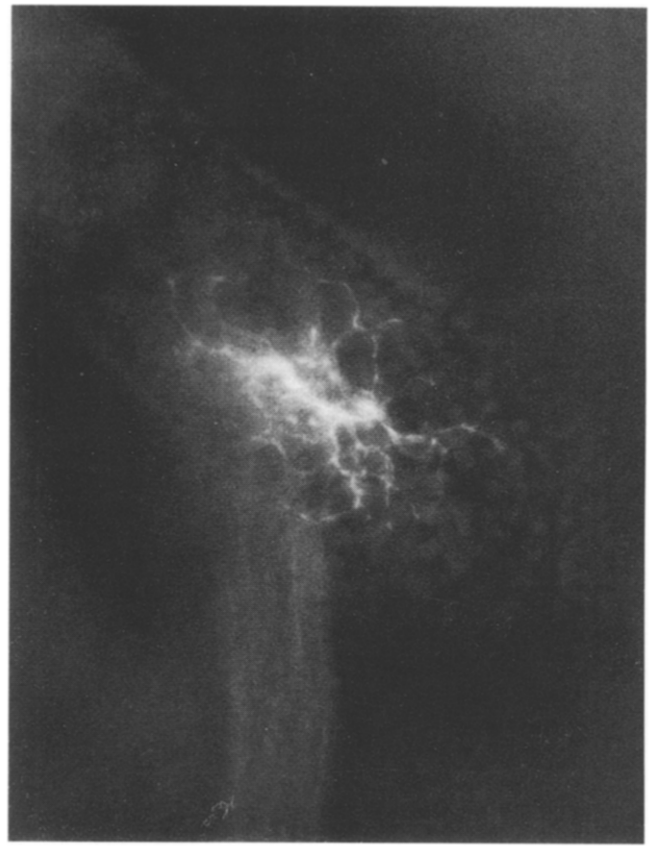

Fig. 6. Photomicrograph of the Lucifer Yellow fluorescence of a large field 'isthmus' afferent innervating the horizontal canal crista (see Fig. 4I). The primary dendritic branch diameters were no more than twice that of the peripheral branch diameters. The extent of fluorescence of central portions of the arbor is exaggerated in the micrograph due to the plane of focus.

Afferent response gain

Of the 8 dye-filled afferent axons in which evoked responses were also studied, a clear dichotomy of sensitivities existed between large- and small-field neurons. Two of the three large-field afferent neurons had gains to a 0.5-Hz stimulus of approximately 20 spikes/s per deg/s (sp/s/d/s) with CVs of 0.61 and 0.75. The other unit (6C) was recorded from a frog in which the animal's physiological state had deteriorated during the experiment (i.e. blood flow within vessels on the VIIIth nerve and brain stem became markedly slower over time). That the afferent response was effected was evident from the unit's unstable resting activity (>7 spikes/s initially to 1.3 spikes/s at the end of the experiment) as well as declining responsiveness of the unit to sinusoidal stimulation. Still the response gain was over 8 sp/s/d/s (CV = 0.69). All

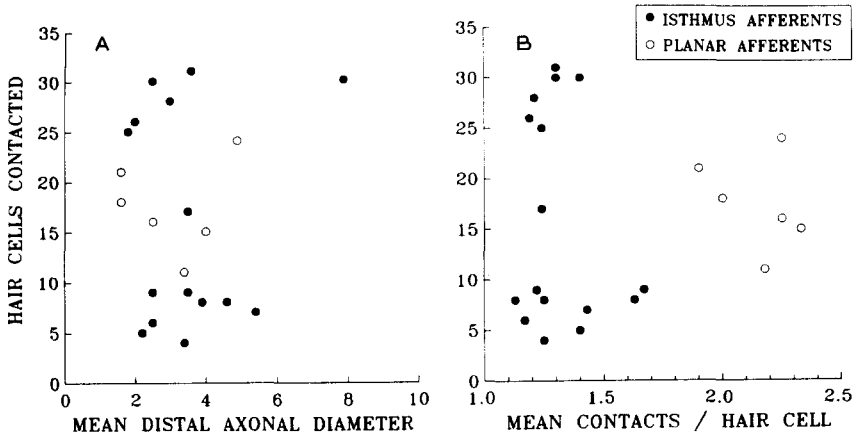

Fig. 7. A: graph showing no apparent correlation between afferent axonal diameter and the number of hair cells innervated. B: graph showing dichotomy in the number of apparent contacts per innervated hair cell between isthmus and planar afferents.

other units reported here had stable resting spike rates and stable response gains over the 2–3 min of recording at each stimulus frequency. The 4 small-field isthmus units (6D–G) had gains of 3.9, 1.6, 3.6 and 2.4 sp/s/d/s, respectively. The remaining unit, mentioned earlier, had a more peripheral planar boundary arbor (6H) and the lowest gain of 0.4 sp/s/d/s. However, this unit was unusual in having a very low spontaneous spike rate (0.8 spikes/s). Units 6D-G were more alike with spike rates (in order) of 10, 4, 4 and 11 spikes/s and coefficients of variation of 0.64, 0.80, 0.64 and 0.62. Of these 4, the unit with the lowest gain had the most centrally located arbor, without any other remarkable features to distinguish it from the other 3 SFA afferent axons.

In studies of vestibular afferent neurons, afferent response gain is often equated with afferent sensitivity. Transducer engineers distinguish the sensitivity of a sensor from its gain by combining the measures of a sensor's gain and its 'noise' into a single quantitative measure such as NEI. For vestibular afferent axons, noise is reflected in the variability of the spontaneous spike production. If the spontaneous spike rate were absolutely constant, then even the smallest stimulus-induced changes in spike activity would be detectable. Since the spontaneous spike rate is not constant, stimulus-induced changes could be confused with noise-induced variations. To quantify the noise-induced variation, we measure its RMS amplitude, which we take to be the RMS amplitude of the variation of the spontaneous ISR about its mean. The sensitivity of a sensory axon can be quantified in terms of the stimulus amplitude (NEI) that is just large enough to produce a spike-rate change equal to the RMS noise-induced spike-rate variation. The RMS variation of the spontaneous spike rate of the irregularly discharging canal afferent axons presented in this paper ranged from 7.6 to 23 spikes/s (mean = 14.4, S.D. = 4.3, n = 17). The mean NEI was 3.2°/s, however, as shown in Fig. 8, there was a progressive reduction in the NEI (i.e. the effective sensitivity increased) as individual afferent response gains increased. The NEI of units with gains >10 sp/s/d/s fell

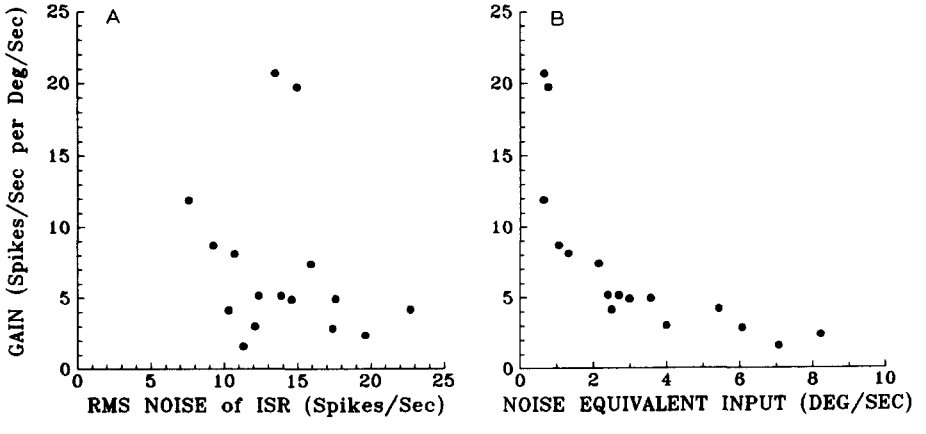

Fig. 8. A: graph showing range of the RMS noise of the ISR for irregularly discharging afferents. High-gain afferents were not differentiated from low-gain afferents by the RMS noise of their resting spike activity. B: graph showing dependence of the noise equivalent input measure on an afferents response gain.

within a relatively narrow range, 0.63–0.76°/s (mean = 0.68, S.D. = 0.07, n = 3) compared to 1.5–8.9°/s (mean = 3.8, S.D. = 2.2, n = 13) for lower gain units. The NEI of regularly discharging, low CV, units could not be determined in the present study because evoked responses from regularly discharging afferent axons were not investigated. However, it is possible to estimate the NEI of regularly discharging afferent fibers (see Materials and Methods section) using data reported by Honrubia et al.[13]. From these data, estimates of the RMS noise in the background firing rate ranged from 1 to 8 spikes/s with most units clustering around 4 spikes/s. The gains reported by Honrubia et al. for this subset of canal afferent neurons (CVs < 0.35) averaged 1.5 sp/s/d/s. Based on these values for gain and RMS variation of the ISR, estimates of NEIs ranged from 1 to 4 with a mean NEI of about 2.7°/s, which is close to the overall mean NEI for irregular canal afferent neurons of 3.2°/s.

DISCUSSION

Li and Lewis[14] characterized the 2 hair cell tuft types described by Hillman[10] as either mature or immature types. Re-examination of hair cell tufts along the crista of the bullfrog revealed a subdivision of the 'mature' hair cell tufts into A and B types as described by Flock and Orman in a study of the grass frog[4]. As a further clarification of the literature, our results differ from those of Suzuki et al.[21] who reported that hair cell stereocilia of the bullfrog crista were longer in the peripheral regions than in the central regions. This is known to be true for mammalian cristae[15]. However, our study indicates that the opposite is true in the bullfrog, which is consistent with Flock and Orman's findings in the grass frog. The bullfrog crista may differ from the grass frog in that the most central portion of the isthmus (torus region) was occupied almost exclusively with type A tufts while the remainder of the isthmus contained a greater mix of types A and B tufts. This tuft distribution and differences in hair cell densities allows the bullfrog crista to be subdivided into 3 epithelial zones: zone I, comprising the planar expansions with roughly twice the hair cell density of the other subdivisions and populated primarily by type B tufts; zone II, comprising the adjacent portions of the isthmus region, populated by a mix of type A and B tufts; and zone III, comprising the torus region, populated by type A tufts.

Do afferent arbors respect the boundaries of these regions? The answer to this question is generally yes for planar vs. isthmus distributions, but within the isthmus, afferent arbors often crossed the boundary between zones II and III. Functional distinctions between planar and isthmus regions are well known and include: generally lower spontaneous activity, higher CVs, generally higher gains and more responsiveness to the velocity of cupular deflection by neurons innervating the isthmus region[1,11,13]. No similar distinctions have been found between isthmus subdivisions.

Although the sample size was small for correlation of evoked responses and afferent arborizations (8 units), our data indicate that afferent response gain withing the isthmus region was higher for afferent neurons innervating a large number of hair cells. Previous studies in the frog have correlated afferent response gain with general arbor location along the crista but were unable to obtain sufficient anatomical detail in the dye-filled arbors to distinguish between high and low gain units innervating similar regions of the crista[11,13]. In mammalian studies, correlations between afferent responses and arborizations are complicated because of the presence of 2 types of nerve endings. The irregularly discharging, central crista afferent axons of bullfrogs are physiologically similar to the irregularly discharging dimorphic afferent axons characterized by Baird et al. in the chinchilla[1]. These studies found that the response gains of dimorphic units are governed to a large degree by post-spike recovery processes of afferent synapses and not by quantitative morphological aspects of the afferent arborizations[1]. This post-spike recovery process was quantified in terms of a sensitivity to galvanic stimulation and correlated with both afferent response gain and CV. Post-spike recovery processes probably play an important role in the response gains of bullfrog afferent axons as well. Why then did the degree of arborization appear to be an important factor in the frog and not in the chinchilla? Perhaps it is due to the greater range of arbor sizes in the dye-filled irregular axons in the frog as compared to those in the chinchilla.

In agreement with previous studies in the bullfrog, afferent response gain did not correlate with axonal diameter[13]. However, the arborization patterns demonstrated with Lucifer Yellow in the present study appear to be generally more extensive and elaborate in their branchings than those of HRP-filled afferent axons reported by Honrubia et al.[13]. Some of the differences may be methodological; however, some differences may relate to the different afferent fiber classes examined in each study. Honrubia et al. examined dendritic arbors of large (>7 μm) and very small (<3 μm) diameter fibers. The afferent axons in the present study were generally of the middle range fiber diameters (2.3–6 μm when myelin sheath thickness is included). Only 3 Lucifer Yellow dye-filled axons exceeded 7 μm in fiber diameter (see Fig. 5B,E,F). Still, none of these had the claw-like character observed by Honrubia et al. to be generally characteristic of the large diameter fibers.

The basic principles behind the semicircular canal organs as inertial motion sensors are well understood[22]. However, when the outputs of these biological sensors have been examined closely, the individual afferent neurons have displayed a great diversity of response characteristics. With respect to response gains, frog canal afferent axons display at least a 50-fold range in gains relative to rotational velocity.

Various aspects of bullfrog crista morphology have been examined in detail by Hillman[8–10] and Li and Lewis[14] with additional studies of afferent morphology Dunn[2], and morphology/physiology by Honrubia et al.[11–13]. Taken together, these studies have indicated that afferent response gain is higher for fibers innervating the central or isthmus portion of the crista as compared to fibers innervating the 'peripheral' or planar regions. However, when afferent sensitivity is quantified in terms of NEI, the rotational sensitivities of isthmus and planar units were quite similar on average. If sensitivity to a rotational stimulus is not an important discriminator between central and peripheral crista afferent neurons, then other differences in response characteristics, particularly phase, are probably of greater functional significance (e.g. their relative responsiveness to the rotational acceleration vs. rotational velocity of the stimulus at frequencies above 0.5 Hz).

Acknowledgements. We would like to thank Dr. Michael Sneary and Mrs. Eva Poinar for their technical assistance and advice on various aspects of this research. This research was supported by NASA Grant NAG 2-448.

REFERENCES

1 Baird, R.A., Desmadryl, G., Fernandez, C. and Goldberg, J.M., The vestibular nerve of the chinchilla, II. Relation between afferent response properties and peripheral innervation patterns in the semicircular canals, *J. Neurophysiol.*, 60 (1988) 182–203.
2 Dunn, R.F., Nerve fibers of the eighth nerve and their distribution to the sensory nerves of the inner ear in the bullfrog, *J. Comp. Neurol.*, 182 (1978) 621–636.
3 Fernandez, C., Baird, R.A. and Goldberg, J.M., The vestibular nerve of the chinchilla, I. Peripheral innervation patterns in the horizontal and superior semicircular canals, *J. Neurophysiol.*, 60 (1988) 167–181.
4 Flock, A. and Orman, S., Micromechanical properties of sensory hairs on receptor cells in the inner ear, *Hearing Res.*, 11 (1983) 249–260.
5 Gacek, R.R. and Rasmussen, G.L., Fiber analysis of the statoacoustic nerve of guinea pig, cat, and monkey, *Anat. Rec.*, 139 (1961) 455–463.
6 Goldberg, J.M. and Fernandez, C., Physiology of pheripheral neurons innervating semicircular canals in the squirrel monkey, I. Resting discharge and response to constant angular accelerations, *J. Neurophysiol.*, 34 (1971) 635–660.
7 Goldberg, J.M. and Fernandez, C., Conduction times and background discharge of vestibular afferents, *Brain Research*, 122 (1977) 545–550.
8 Hillman, D.E., Cupular structure and its receptor relationship, *Brain Behav. Evol.*, 10 (1974) 52–68.
9 Hillman, D.E., Morphology of peripheral and central vestibular systems. In R. Llinas and W. Precht (Eds.), *Frog Neurobiology*, Springer Verlag, Berlin, 1976, pp. 452–480.
10 Hillman, D.E., Relationship of the sensory cell cilia to the cupula, *Scanning Electron Microsc.*, 2 (1977) 415–420.
11 Honrubia, V., Sitko, S., Kimm, J., Betts, W. and Schwartz, I., Physiological and anatomical characteristics of primary vestibular afferent neurons in the bullfrog, *Int. J. Neurosci.*, 15 (1981) 197–206.
12 Honrubia, V., Sitko, S., Lee, R., Kuruvilla, A. and Schwartz, I., Anatomical characteristics of the anterior vestibular nerve of the bullfrog, *Laryngoscope*, 94 (1984) 464–474.
13 Honrubia, V., Hoffman, L.F., Sitko, S. and Schwartz, I.R., Anatomic and physiological correlates in bullfrog vestibular nerve, *J. Neurophysiol.*, 61 (1989) 688–701.
14 Li, C.W. and Lewis, E.R., Structure and development of vestibular hair cells in the larval bullfrog, *Ann. Otol. Rhinol. Laryngol.*, 88 (1979) 427–437.
15 Lim, D.J., Ultra anatomy of sensory end-organs in the labyrinth and their functional implications. In G.E. Shambaugh and J.J. Shea (Eds.), *Proceedings of the Shambaugh Fifth International Workshop on Middle Ear Microsurgery and Fluctuant Hearing Loss*, The Strode Publishers, Huntsville, AL, 1977, pp. 16–27.
16 Lindeman, H.H., Studies on the morphology of the sensory regions of the vestibular apparatus, *Ergebn. Anat. Entwicklungsgesch.*, 42 (1969) 1–113.
17 McLaren, J.W. and Hillman, D.E., Displacement of the semicircular canal cupula during sinusoidal rotation, *Neurosience*, 4 (1979) 2001–2008.
18 Myers, S.F. and Lewis, E.R., Microrotational responses of vestibular afferents in the bullfrog, *Brain Research*, (1990) submitted.
19 Smith, C.E. and Goldberg, J.M., A stochastic afterhyperpolarization model of repetitive activity in vestibular afferents, *Biol. Cybern.*, 54 (1986) 41–51.
20 Stewart, W.W., Functional connections between cells as revealed by dye-coupling with a highly fluorescent naphthalamide tracer, *Cell*, 14 (1978) 741–759.
21 Suzuki, M., Harada, Y. and Sato, S., An experimental study on the isolated lateral semicircular canal of the bullfrog, *Arch. Oto-Rhino-Laryngol.*, 243 (1986) 27–30.
22 Wilson, V.J. and Melville Jones, G., *Mammalian Vestibular Physiology*, Plenum, New York, 1979, 365 pp.